Supporting Information Appendix

Table of contents

Fig S12. | Morphology observation for Li/C-wood and bare Li metal electrodes after stripping and plating back 3 mAh cm^{-2} of Li.

Part III: Supplementary Table

Table S1. | Overpotential comparison of bare Li metal electrodes and Li/C-wood electrodes at different current densities

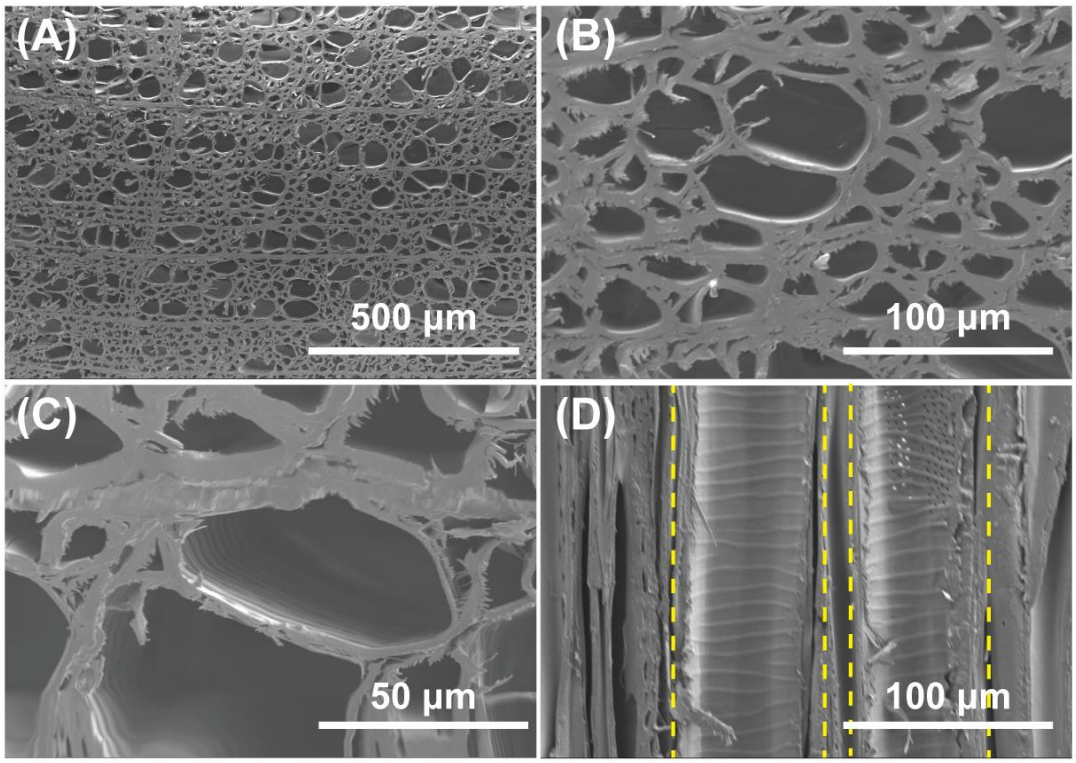

Fig. S1. Morphology study of pristine basswood presents the typical porous structure and natural channels with sizes ranging from 15 μm to 76 μm. (*A*-*C*) Top-view SEM images at various magnifications; (*D*) a cross-sectional SEM image of basswood shows a detailed microstructure on the walls of channels.

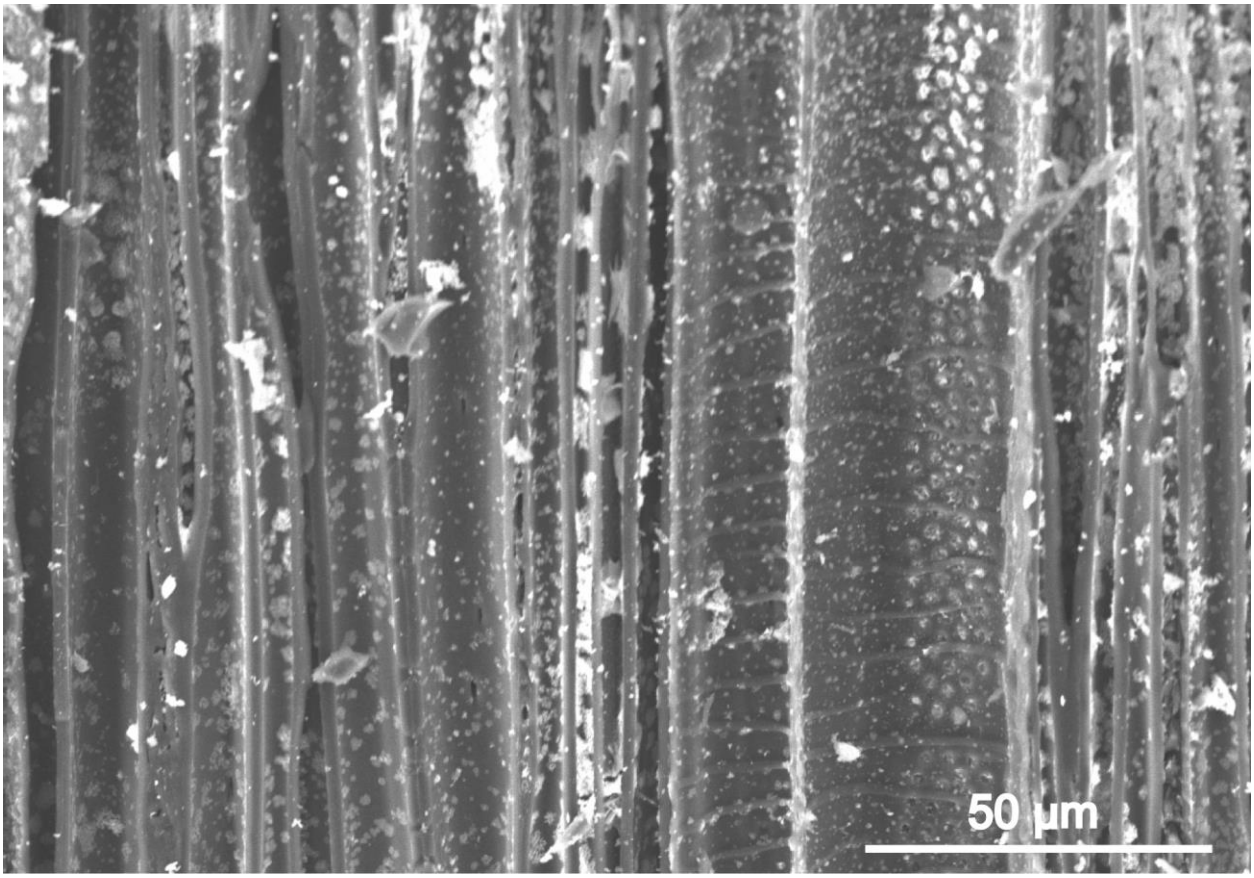

Fig. S2. Cross-sectional SEM image of ZnO coated C-wood, showing that ZnO particles formed inside the C-wood channels. The ZnO particles promote the wetting property between Li metal and C-wood.

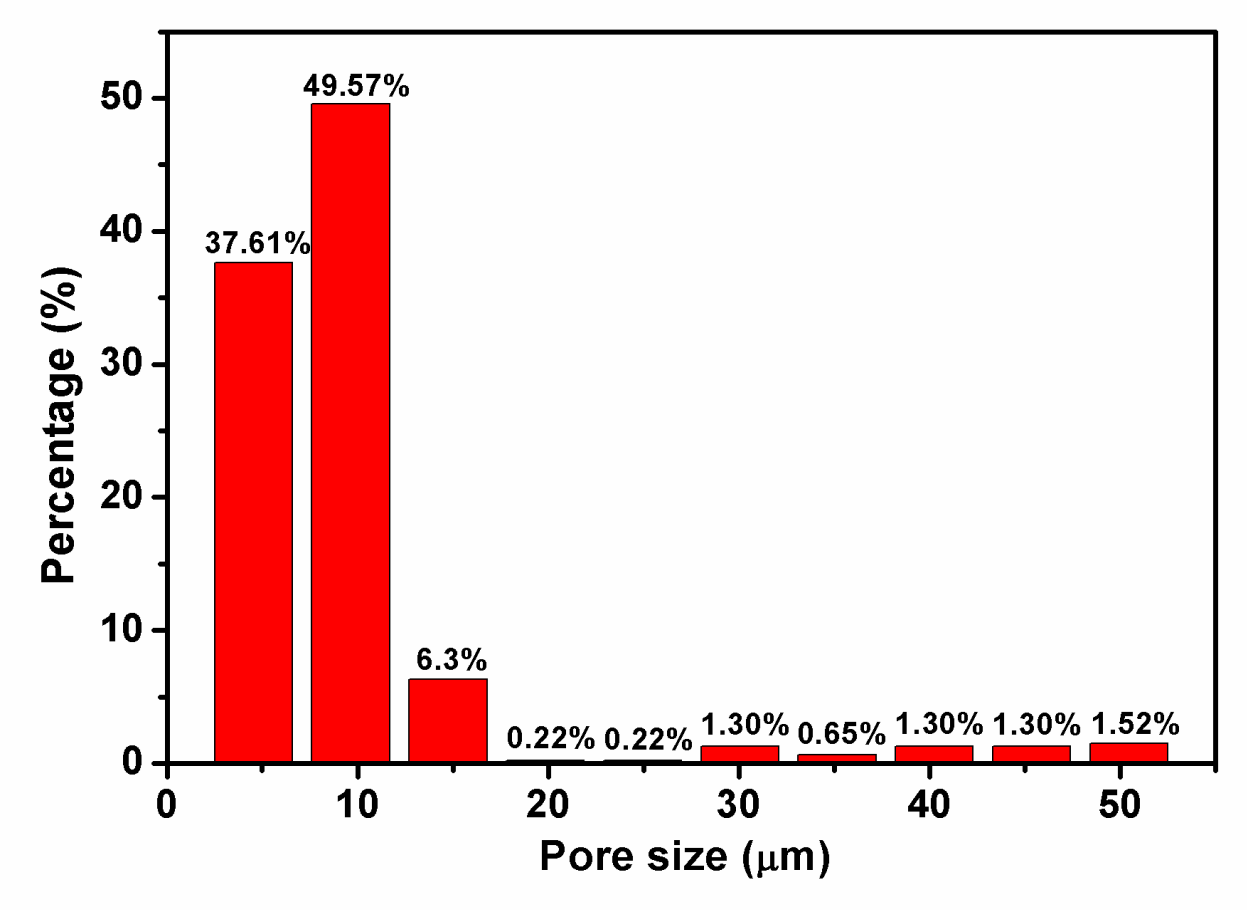

Fig. S3. The pore size distribution of C-wood, revealing that 87% of the pore size ranges from 2.0 to 12.2 μm.

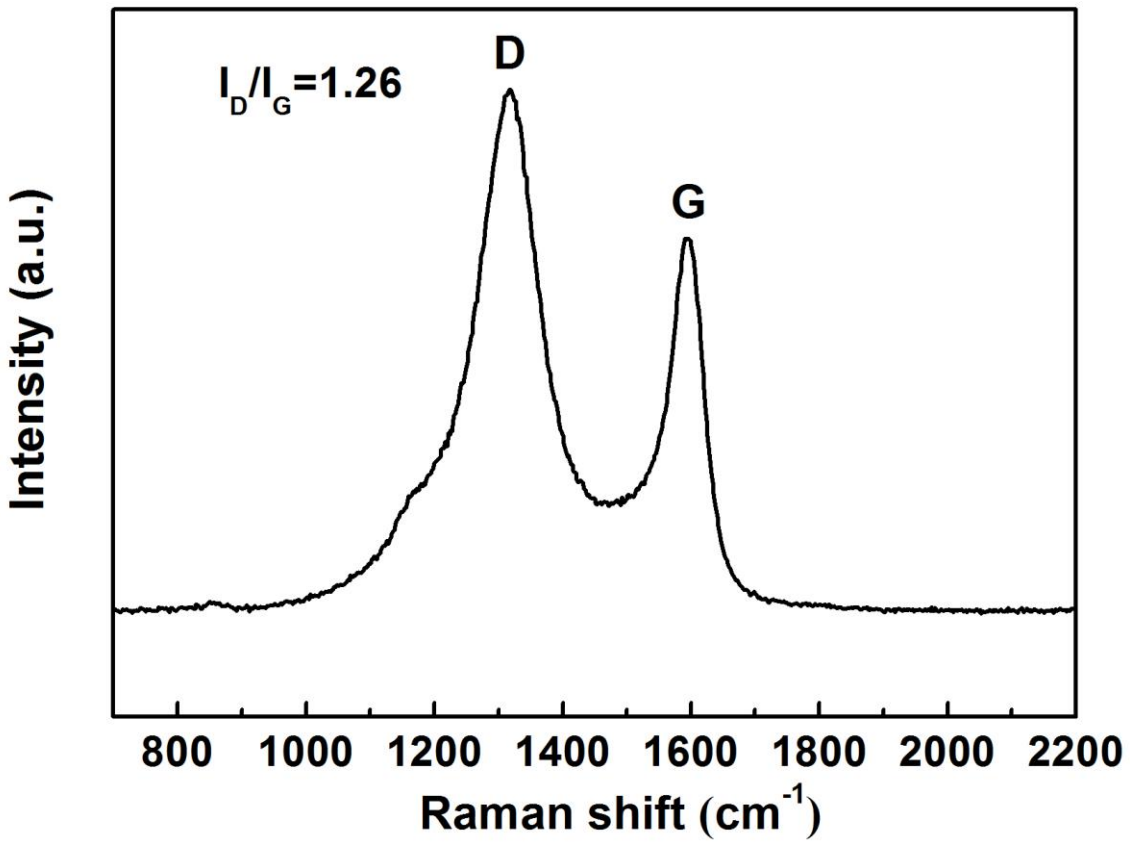

Fig. S4. Raman spectra of the C-wood, where D peak and G peak locate at 1316 cm^{-1} and 1596 cm^{-1}, respectively. The dispersion of G peak and the little dispersion of D peak related to the stretching motion of sp2 structures are good indicators of disorder. The intensity ratio of I(D)/I(G) from Raman spectra is 1.26 which confirms the amorphous feature of the C-wood.

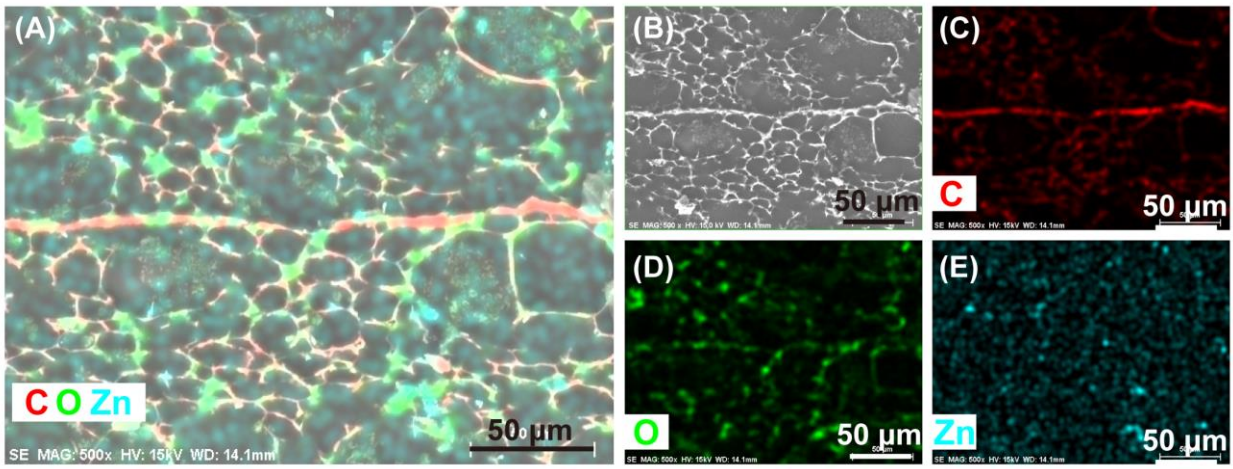

Fig. S5. Top-view SEM micrographs of the Li/C-wood composite with EDX mapping. (*A*) Overlapped elemental mapping images of C, O, and Zn. (*B*) Corresponding top view SEM image. (*C-E*) Individual elemental maps of (*C*) C, (*D*) O, and (*E*) Zn.

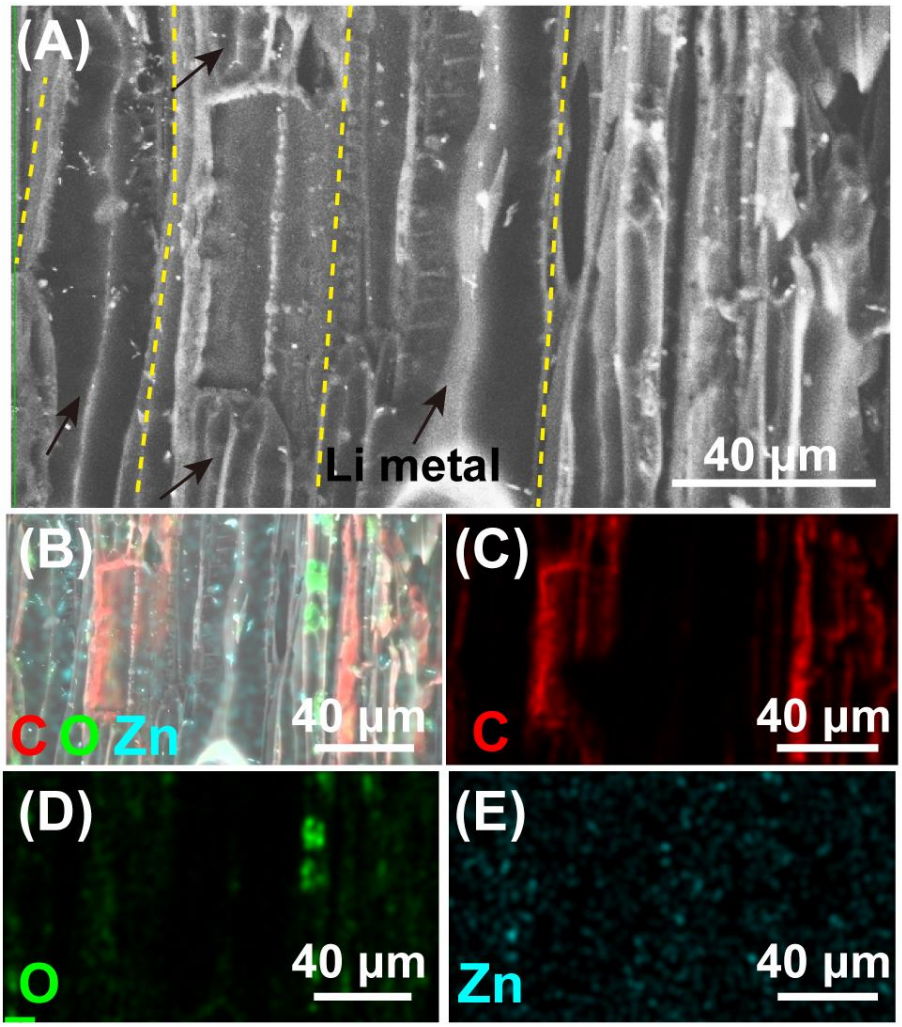

Fig. S6. Cross-sectional SEM micrographs and EDX mapping of the Li/C-wood composite with EDX mapping. (*A*) SEM image of Li/C-wood composite with aligned channels. (*B*-*E*) Representative elemental maps from EDX analysis based on SEM for (*B*) overlapped mapping of C, O, and Zn, (*C*) C, (*D*) O, and (*E*) Zn.

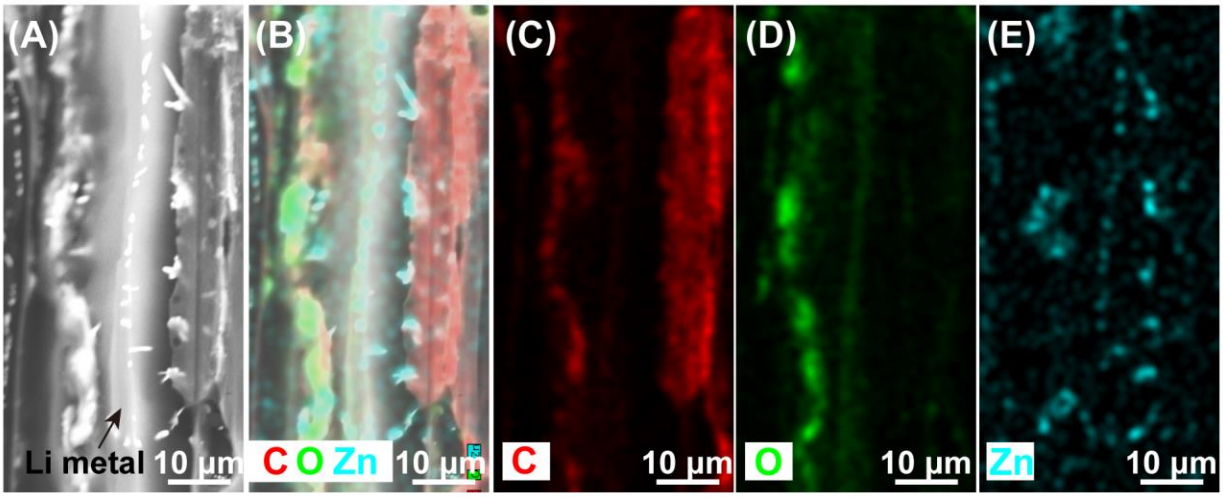

Fig. S7. Cross-sectional SEM micrographs and EDX mapping images of an individual channel. (*A*) SEM image of an individual channel infused by Li metal. (*B-E*) Corresponding elemental mapping for (*B*) overlapped mapping of C, O, and Zn, (*C*) C, (*D*) O, and (*E*) Zn.

The cross-sectional view of the Li/C-wood electrodes exhibits Li metal within the inner spaces of the aligned wood channels. Overlapped and individual elemental maps of C, O and Zn further confirmed the arrangement of Li metal in the aligned wood channels. The C signals are found in EDX mapping at the sites of the channel walls of carbonized wood. Both the SEM and EDX images confirm the unique low tortuosity feature of this novel Li metal anode.

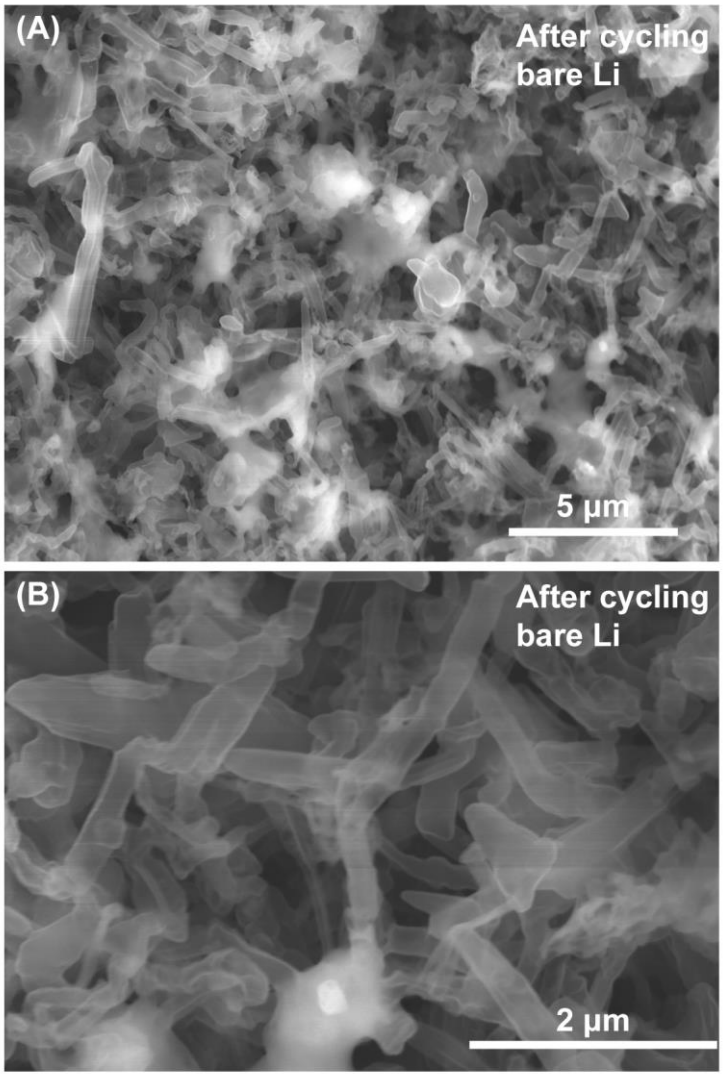

Fig. S8. (*A*, *B*) Different magnifications of bare Li metal electrode after cycling at 1.0 mA cm^{-2} with a capacity of 1 mAh cm^{-2}, showing a dendritic morphology.

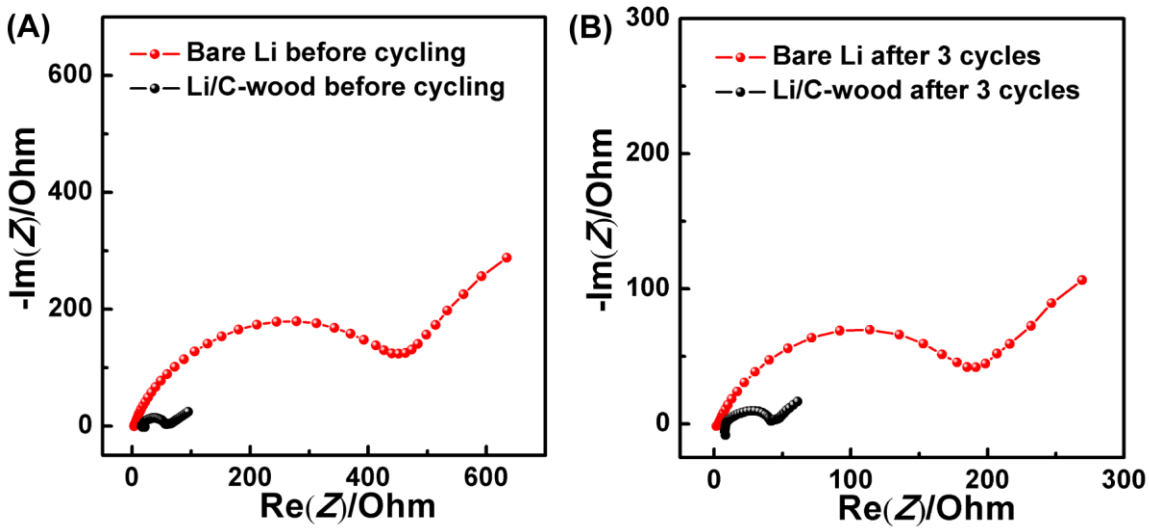

Fig. S9. Electrochemical impedance spectra comparison of symmetrical cells using bare Li and Li/C-wood electrodes before cycling (*A*) and after 3 cycles (*B*). In contrast to the bare Li cells, the small charge transfer resistance of the Li/C-wood cell indicated fast kinetics of electrochemical reaction at the interface between electrode and electrolyte.

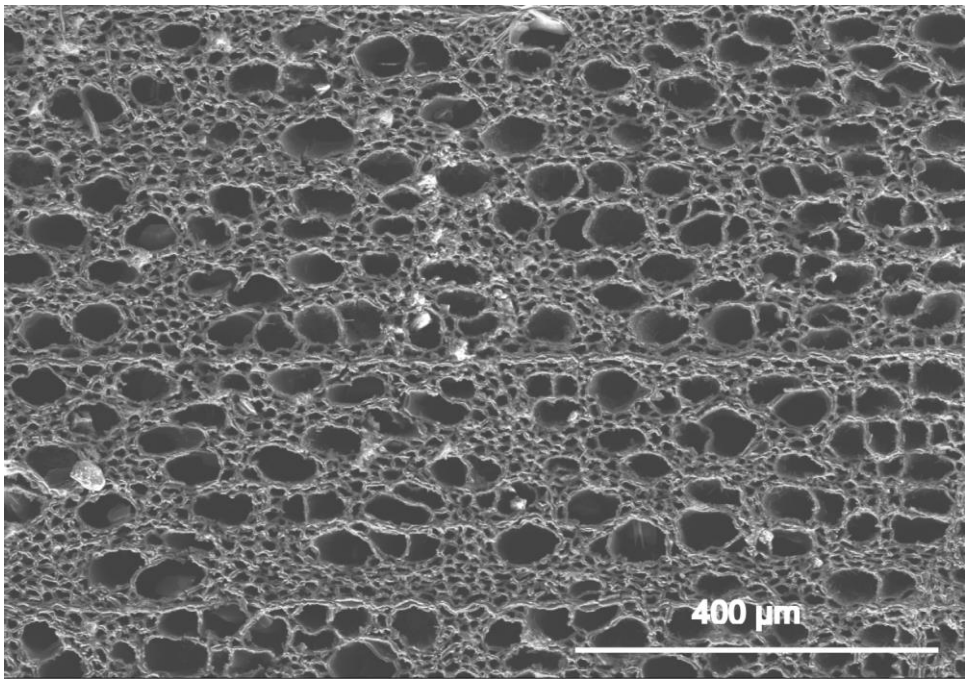

Fig. S10. A top-view SEM image of Li/C-wood electrode after removing Li from Li/C-wood electrode with a capacity of 875 mAh g^{-1} under the current density of 1 mA cm^{-2}. The total capacity of Li/C-wood composite is about 2650 mAh g^{-1}, which corresponds to one third of the Li in the C-wood channels being removed from Li/C-wood composite.

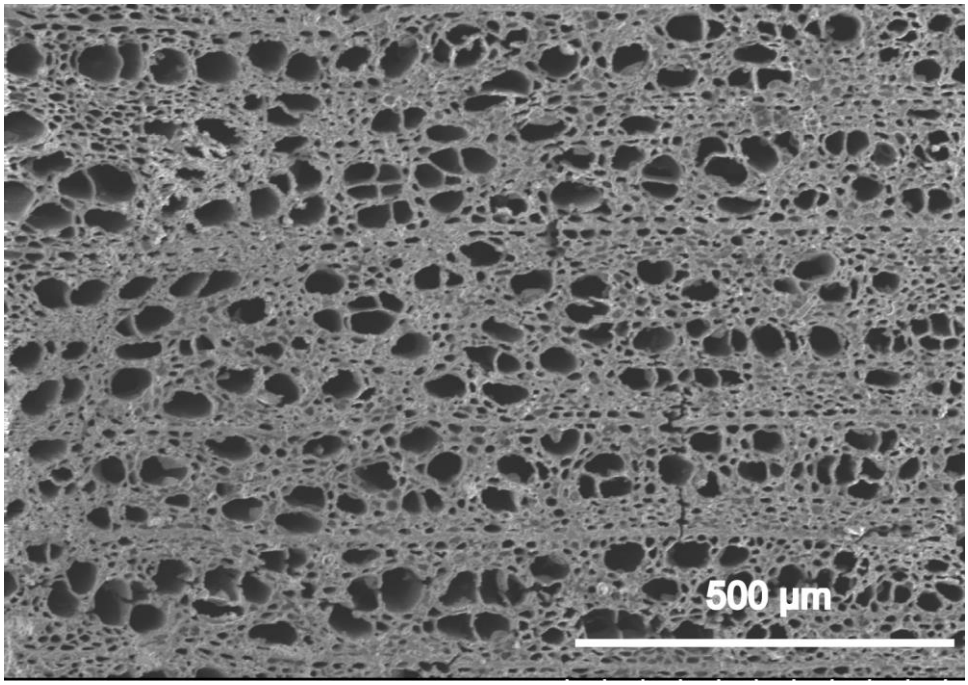

Fig. S11. A top view SEM image of Li/C-wood electrode after stripping all of the Li out at 1 mA cm^{-2}. Compared with Fig. 3*G*, the surface of Li/C-wood presents a hollow-structure, which indicates the removal of Li from Li/C-wood composite after stripping.

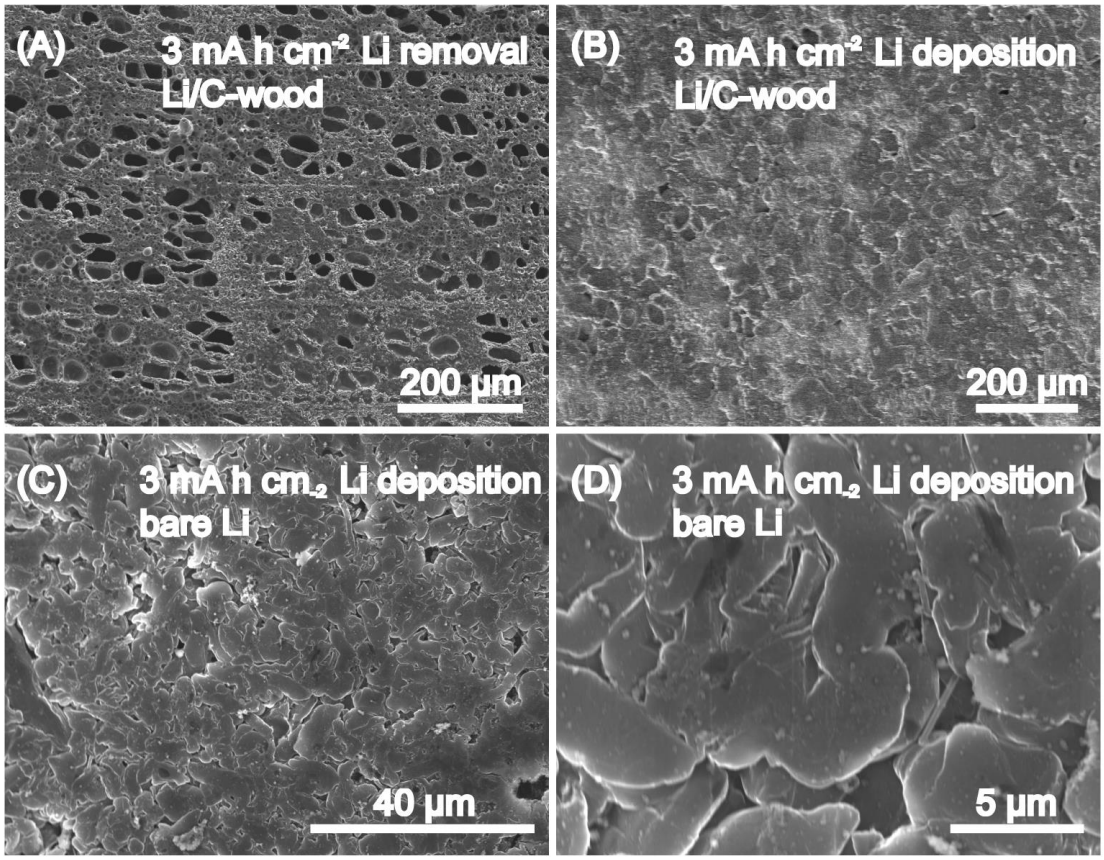

Fig. S12. Morphology observation for Li/C-wood and bare Li metal electrodes. Top view SEM images of Li/C-wood electrode (*A*) after stripping 3 mAh cm^{-2} of Li and (*B*) after plating back 3 mAh cm^{-2} of Li at 1 mA cm^{-2}. (*C*, *D*) Different magnifications of the bare Li metal electrode after a full stripping/plating cycle with a capacity of 3 mAh cm^{-2} at 1 mA cm^{-2}, showing a mossy surface with Li dendrites.

Table S1. Overpotential comparison of bare Li metal electrodes and Li/C-wood electrodes at different current densities

Electrode	0.5 mA cm^{-2}	1 mA cm^{-2}	3 mA cm^{-2}
Bare Li metal	64 mV	83 mV	173 mV
Li/C-wood	22 mV	53 mV	104 mV